Predicting Fatigue Crack Retardation in 7150 Aluminum Alloy

Marcos Venicius S. Pereira[1,a], Fathi Aref Darwish[2,b], Leonardo B. Godefroid[3,c] and Arnaldo F. Camarão[4,d]

[1] Department of Materials Science and Metallurgy / PUC-Rio

Rua Marquês de São Vicente 225, Rio de Janeiro / RJ, CEP 22453-900 - Brazil

[2] Department of Civil Engineering / UFF

Rua Passo da Pátria 156, Niterói / RJ, CEP 24210-240 - Brazil

[3] Metallurgy and Materials Science Department / UFOP

Campus Universitário / Escola de Minas, Ouro Preto / MG, CEP 35400-000 - Brazil

[4] Product Engineering / ArvinMeritor Osasco

Av. João Batista 825, Osasco / SP, CEP 06097-900 - Brazil

[a]marcospe@puc-rio.br, [b] fadarwish@poscivil.uff.br, [c]leonardo@demet.em.ufop.br and [d]arnaldo.camarao@arvinmeritor.com

Keywords: crack propagation kinetics, crack retardation models, fatigue life extension.

Abstract. The aim of this work is to evaluate the applicability of the Wheeler and Willenborg models to predicting fatigue crack growth retardation in a 7150 overaged aluminium alloy used as aircraft structural material. Constant amplitude loading was adopted for the fatigue tests making use of CT specimens. Three different single tensile overloads were applied at a given crack length during CA fatigue loading and crack growth rate da/dN versus the stress intensity factor range ΔK was monitored, evidencing the retardation in crack propagation over an interval of crack length. The results indicated that the fatigue life increases with the increase in the magnitude of overloading. The size of the delay zone as well as the retarded crack propagation rate were predicted by both the Wheeler and Willenborg models and then compared with the experimental data. Finally, the results are presented and discussed focusing on the comparison between the predictions made by the two models in light of the experimental data.

Introduction

Structural and mechanical components when in service under cyclic loading may be subjected to either variable amplitude loading or occasional overload cycles and these load interactions complicate life prediction. Sometimes, overloads are purposely applied to produce some beneficial effects on the fatigue resistance of the components and it has been known for over forty years that overload cycles of sufficient magnitude can result in a transient retardation in the rate of fatigue crack growth at the baseline level [1]. It is also well established that this retardation is closely related to the residual compressive stress field induced in the vicinity of the crack tip [2]. Following an overload cycle, the fatigue crack starts to advance into the overload (OL) plastic zone and the residual compressive stresses in an element just behind the crack tip are relaxed. This contributes to the level of crack closure in the wake of the crack tip, thus retarding fatigue crack propagation. As the crack exits the OL plastic zone, the propagation rate is generally back again at the baseline level corresponding to the constant amplitude (CA) loading. Other retardation mechanisms such as crack blunting and strain hardening of the material within the OL plastic zone can be activated following overloading and therefore contribute to the extension of fatigue life.

The magnitude and extent of crack growth retardation due to the imposition of a single OL during CA cycling are usually measured by parameters such as the delay cycles number N_d and the

delay zone size Δa_d. The first parameter refers to the increase in residual fatigue life due to overloading and the second is a measure of the OL affected crack length increment along which retardation takes place. Both N_d and Δa_d can vary depending on load parameters [3]. For example, the higher the ratio between the magnitude of the overload and that of the CA maximum load, R_{OL}, the more pronounced the crack growth retardation. That is, an increase in R_{OL} results in an increase in N_d and Δa_d, as well as in a decrease in the minimum da/dN level [3]. For high overloads (R_{OL}=2.5) the initial crack growth acceleration that immediately follows an overload was absent and immediate retardation was observed [4,5].

Starting early seventies, a large number of models which incorporate interaction effects have been introduced for predicting fatigue crack growth under variable amplitude (VA) loading [6-11]. These models are characterized by introducing crack tip plasticity effects and they comprise three distinct groups. The yield zone models are based on considerations on the size of monotonic plastic zone created at the crack tip due to an OL and do not take into account plasticity induced crack closure due to the imposition of the overload. Crack closure models, on the other hand, represent an improvement of the more primitive yield zone models and take into consideration the closure behavior based on crack closure measurements made during CA loading [12]. Assumptions are then made about the crack closure behavior under VA loading. In the more sophisticated strip yield models, the occurrence of plasticity induced crack closure is calculated rather than estimated from measurements made during CA loading [12].

The present study has the purpose of applying two of the yield zone models, namely the Wheeler and Willenborg models, in order to evaluate fatigue crack growth retardation in a 7150 T7 aluminum alloy developed for aeronautic applications after a single overload cycle applied at a given crack length during CA loading. The study was motivated by the simplicity of the two models in question and was primarily aimed at comparing the delay parameters predicted by their application with experimental data.

Fatigue Crack Growth under Variable Amplitude Loading

The model proposed by Wheeler [6] represents an approach to explain crack growth delays caused by high loads. The model recognizes that new plastic zones are created inside the large monotonic plastic zone of an overload. A crack growth retardation factor γ, which is related to the sizes of both the cyclic and monotonic plastic zones, was then introduced by Wheeler, making it possible for one to predict crack growth rate within the delay zone, $(da/dN)_{VA}$, from the expression:

$$(da/dN)_{VA} = \gamma\,(da/dN)_{CA}\,. \tag{1}$$

According to this model, the retardation factor γ is assumed to be a power function of the ratio r_p/λ, where r_p is the current plastic zone size corresponding to a given crack length a and λ the distance between the crack tip and the edge of the OL plastic zone as presented in Fig. 1.

Thus γ can be expressed as:

$$\gamma = (r_p/\lambda)^m \tag{2}$$

where the exponent m is an empirical constant dependent on the type of the VA load history.

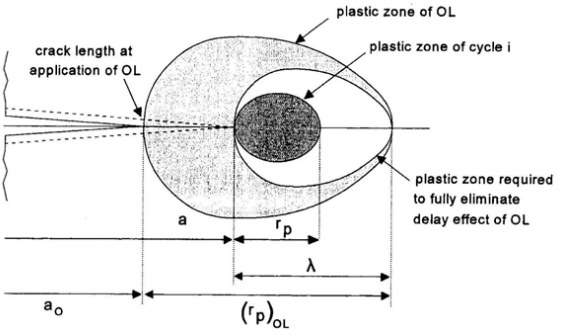

Figure 1. Plastic zone size definitions used in the model of Wheeler, corresponding to a generic cycle *i* [12].

Assuming plane stress loading conditions, the current plastic zone size r_p can be calculated from the expression below:

$$r_p = \frac{1}{\pi}\left(\frac{K_{\max}}{\sigma_Y}\right)^2 \tag{3}$$

where $K_{\max}$ is the maximum stress intensity factor corresponding to the CA loading for a crack length a and σ_Y is the yield stress. For a crack length a, λ is given by the expression:

$$\lambda = a_0 + (r_p)_{OL} - a \tag{4}$$

where a_0 is the crack length at which the overload was applied and $(r_p)_{OL}$ is the overload plastic zone size, that can be calculated, assuming plane stress loading, using the following expression:

$$(r_p)_{OL} = \frac{1}{\pi}\left(\frac{K_{OL}}{\sigma_Y}\right)^2 \tag{5}$$

where K_{OL} is the OL stress intensity factor. At this point, it is important to mention that both $K_{\max}$ and K_{OL} can be calculated from the corresponding loads $P_{\max}$ and P_{OL} using relations documented in the appropriate literature [7,13].

As the crack propagates through the delay zone, r_p becomes larger whereas λ gets smaller. As a result, γ will increase gradually from its minimum value $\gamma_{\min}$ to a maximum value of unity as the far edge of the current plastic zone starts to exit the OL plastic zone and the delay effect would thus be gone. With this in mind, one can estimate, from the following relation, the fatigue crack length over which the delay effect does in fact act, i.e., the delay zone length Δa_d^*:

$$\Delta a_d^* = (r_p)_{OL} - r^*_p \tag{6}$$

where r^*_p is the size of the current plastic zone which reaches the far edge of the OL plastic zone.

The model proposed by Willenborg [8] is based on the assumption that crack growth delay after an OL is due to a reduction in K_{max}, corresponding to the current crack length. According to the model, the reduction in K_{max}, K_{red}, is given by [8]:

$$K_{red} = K_{req} - K_{max} \tag{7}$$

where K_{req} is the stress intensity factor necessary to produce a plastic zone that extends a distance λ ahead of the advancing fatigue crack tip, to the far edge of the OL plastic zone, as presented earlier in Fig. 1. Under plane stress conditions, K_{req} at a given crack length a can be determined from the expression:

$$K_{req} = \sigma_Y \sqrt{\pi\lambda}\,. \tag{8}$$

The size of the overload plastic zone can be determined from Eq. 8 by substituting K_{OL} for K_{req}. Taking into account the reduction in the stress intensity factor due to overloading, one can define effective values of K_{max} and K_{min} as follows:

$$K_{max,eff} = K_{max} - K_{red} \tag{9}$$

$$K_{min,eff} = K_{min} - K_{red} \tag{10}$$

where K_{min} is related to CA loading.

From the effective stress intensity levels given above, one can, in turn, define in the usual manner the effective stress intensity factor range, ΔK_{eff}, as well as the effective stress intensity factor ratio R_{eff}. At this point, it is important to note that Eqs. 9 and 10 indicate that ΔK_{eff} is equivalent to ΔK. However, according to the Willenborg model, negative values of $K_{min,eff}$ should be taken as null and ΔK_{eff} becomes equal to $K_{max,eff}$ in this case.

Knowing ΔK_{eff} and R_{eff}, the fatigue crack propagation rate $(da/dN)_{VA}$ within the delay zone can be estimated and then related to the corresponding propagation rate at the baseline level $(da/dN)_{CA}$ by the retardation factor γ defined in Eq. 1.

Fatigue crack growth rate under CA loading can be predicted from the relation proposed by Forman and co-workers [14], as shown in Eq. 11 below:

$$\left(\frac{da}{dN}\right)_{CA} = \frac{C(\Delta K)^n}{(1-R)K_c - \Delta K} \tag{11}$$

where C and n are the Paris law material constants and K_c is the material's toughness.

Within the delay zone that follows the application of an OL, the crack propagation rate $(da/dN)_{VA}$ can be calculated by substituting ΔK_{eff} and R_{eff} for ΔK and R in Eq. 11. After passing through the minimum that follows an overload, the retardation factor γ starts to increase and eventually becomes equal to unity, thus restoring the propagation rate back to the baseline level at the end of the delay zone. The basic feature of the Willenborg model, therefore, refers to the fact that crack growth retardation, which follows overloading, ends when the values of ΔK_{eff} and R_{eff} converge to those of ΔK and R. The current crack length, a^*, at which such convergence takes place can thus be determined and the delay zone length Δa_d^* will be given by the difference between a^* and a_0.

Based on Eq. 11, $(da/dN)_{CA}$ and $(da/dN)_{VA}$ can be calculated and the delay factor γ for a given crack length a can, therefore, be expressed as:

$$\gamma = \left(\frac{\Delta K_{eff}}{\Delta K}\right)^{n}\left[\frac{(1-R)K_c - \Delta K}{(1-R_{eff})K_c - \Delta K_{eff}}\right] \tag{12}$$

Experimental Procedure

The material used for this investigation is a 7150 T7 aluminum alloy developed for aeronautic applications [15]. The alloy, which contains, in weight percent, 6.6% Zn, 2.3% Mg, 2.1% Cu, 0.1% Zr, 0.05% Fe, 0.05% Ti, 0.03% Si and traces of Mn and Cr, was received in the form of an extruded T-profiled rod. The alloy yield stress, σ_Y, determined along the L direction amounts to 565 MPa and its L-T fracture toughness, K_{Ic}, is situated at 24 MPa$\sqrt{m}$.

Compact tension (CT) specimens were machined along the L-T orientation, in accordance with the ASTM E647-01 recommendation [13]. The specimen width, W, and specimen thickness, B, were taken as 32 and 8 mm, respectively, and a starter notch was machined to a depth of 7 mm. The specimen surfaces were polished and fine lines were drawn parallel to the specimen axis in order to facilitate monitoring crack growth during cyclic loading. Finally, the CT specimens were precracked up to a crack length of 1.5 mm, i.e., to a total a/W of 0.27.

CA cyclic loading was applied to the precracked specimens so as to obtain the typical da/dN versus ΔK curves. The tests were performed at room temperature using a servo-hydraulic machine, operated at a frequency of 20 Hz. The specimens were submitted to a tension-tension mode I loading with a maximum load of 2.1 kN and a load ratio R of 0.3, and fatigue crack length was monitored using a traveling microscope. Overload cycles were applied manually under load control at an a/W ratio of 0.4 by increasing the load to the defined level, going down to the minimum value of 0.63 kN and then returning to the CA loading scheme. The overload ratio R_{OL}, defined by K_{OL} / $K_{\max}$ [16], was taken as 1.5, 1.75 and 2, corresponding to single overload levels of 3.2, 3.7 and 4.2 kN, respectively.

Results and Discussion

Following the application of single overloads during CA fatigue testing, the maximum retardation in crack propagation is reached only after a small crack length increment [12]. After passing the point of maximum retardation, defined by $\gamma = \gamma_{\min}$, da/dN starts to increase and eventually returns, over some crack extension Δa_d, to the normal growth rate at the CA baseline level. The values of Δa_d, together with those of $\gamma_{\min}$, are presented in Table 1 for the three R_{OL} levels considered in this work. The numbers listed in this table indicate, as one may expect, that an increase in the overload ratio is associated with an increase in Δa_d and decrease in $\gamma_{\min}$. This, in turn, is reflected, as Table 1 indicates, in an increase in the delay cycles number N_d and hence in the residual fatigue life.

Table 1. Values of the delay parameters determined experimentally for the different R_{OL} levels

R_{OL}	$\gamma_{\min}$	Δa_d [mm]	N_d
1.50	0.20	0.20	4660
1.75	0.12	0.26	7640
2.00	0.04	0.36	18007

An experimental value of γ, corresponding to a given crack length a within the delay zone, Δa_d, can be used to estimate the exponent m by substituting in Eq. 2 the appropriate r_p and λ values calculated, respectively, from Eqs. 3 and 4. The use of Eq. 3 to calculate r_p implies in assuming plane stress loading conditions. This is considered to be consistent with the fact that measurements

of crack length were made on the specimen surface. The values of m obtained for a given overload ratio were found to vary with the crack length a, giving rise, as can be verified from Table 2, to a considerable degree of scatter. The values of the delay zone size Δa_d^*, estimated from Eq. 6, are listed in the same table in comparison with the values determined from the experimental data Δa_d. The values of $(r_p)_{OL}$ are also included in the same table.

Table 2. Delay parameters Δa_d^* and m as determined for the Wheeler model.

R_{OL}	Δa_d [mm]	Δa_d^* [mm]	$(r_p)_{OL}$ [mm]	m
1.50	0.20	0.14	0.25	2.6 ± 0.7
1.75	0.26	0.23	0.34	2.1 ± 0.8
2.00	0.36	0.33	0.44	0.6 ± 0.25

One can thus conclude that the delay zone measured experimentally agrees fairly well with the calculated value for the three overload levels. The values of m listed in Table 2 can be used to calculate, from Eq. 2, the retardation factor γ at different crack length increments within the delay zone. The values obtained are denoted γ_c and are presented in Table 3 in comparison with their experimental counterparts γ_e. Although γ_c and γ_e are seen to be in fair agreement, it is evident that the use of a unique m value may lead to under- or overstimating the retardation factor as crack propagation proceeds. These observations appear, as pointed out by Schijve [12], to corroborate the limitations of the Wheeler model in predicting the crack growth behavior under VA loading.

The application of the Willenborg model is based on determining the crack length a*, at which ΔK_{eff} and R_{eff} converge to ΔK and R. The values of a* thus obtained are presented in Table 4, together with the corresponding ΔK values, denoted ΔK*, as well as those of Δa_d^* and Δa_d.

As Table 4 indicates, Δa_d^* is in fair agreement with Δa_d and hence one may use the Willenborg model to predict the extent of the delay zone resulting from overloading.

Table 3. Experimental and Wheeler-predicted values of the retardation factor at different crack length increments within the delay zone

R_{OL}	a [mm]	γ_c	γ_e
1.50	12.89	0.39	0.20
	12.90	0.47	0.46
	12.91	0.56	0.64
	12.92	0.70	0.76
	12.93	0.85	0.80
	12.94	1.00	1.00
1.75	12.91	0.22	0.12
	12.92	0.25	0.18
	12.95	0.34	0.70
2.00	13.00	0.63	0.52
	13.02	0.67	0.64
	13.04	0.71	0.76
	13.06	0.76	0.84
	13.08	1.00	1.00

Table 4. Values of a^* and ΔK^* as predicted by the Willenborg model

R_{OL}	a^* [mm]	ΔK^* [MPa$\sqrt{m}$]	Δa_d^* [mm]	Δa_d [mm]
1.50	12.94	7.46	0.14	0.21
1.75	13.03	7.51	0.23	0.28
2.00	13.10	7.56	0.30	0.36

In regard to the retardation factor, predicted by the Willenborg model, the values of γ can be calculated from Eq. 12, taking the Paris law exponent equal to 3.8. Table 5 indicates a fair agreement between the calculated γ_c and experimental γ_e values. However, it is noticed that, whereas the Willenborg model tends to underestimate the retardation factor for the high overload ratio (R_{OL} = 2), the use of the model results in overestimating γ_c for the other two R_{OL} ratios.

Table 5. Experimental and Willenborg-predicted values of the retardation factor

R_{OL}	a [mm]	γ_c	γ_e
1.50	12.90	0.75	0.46
	12.91	0.81	0.64
	12.92	0.87	0.76
	12.93	0.95	0.80
	12.94	1.00	1.00
1.75	12.91	0.24	0.12
	12.92	0.30	0.18
	12.95	0.58	0.70
	13.03	1.00	1.00
2.00	12.94	0.04	0.03
	13.00	0.19	0.52
	13.02	0.31	0.64
	13.04	0.48	0.76
	13.06	0.61	0.84
	13.10	1.00	1.00

Concluding Remarks

The purpose of the present work was to evaluate the applicability of the models proposed by Wheeler and Willenborg to predicting fatigue crack growth retardation in an 7150 T7 aluminum alloy developed for aeronautic applications. From what is presented above, the following remarks can be made:

- An increase in the overload ratio during CA loading results in a more effective crack growth retardation as evidenced by the increase in the extent of the delay zone and by a decrease in the retardation factor.
- The extent of the retardation zone predicted by both the Wheeler and Willenborg models agrees fairly well with the experimental observations.
- The form of the power function proposed by Wheeler for the retardation factor implies in different values of the exponent m as calculated from the experimental data. A single value of that exponent would therefore lead to imprecise estimates of the crack propagation rate along the delay zone.
- The applicability of the Willenborg model to predicting the retardation factor depends on the level of overloading. While, in the present study, this prediction was found to be overestimated for the overload ratio of 1.5, the model underestimates the retardation effect for R_{OL} = 2.

References

[1] J. Schijve, in: *Report No. MP-195*, edited by National Luchtvaart Laboratorium, The Netherlands (1960).

[2] A.J. McEvily and S. Ishihara, in: *Modern Trends on Fatigue*, edited by P.M. Pimenta, L.C.H. Ricardo and A.F. Camarão / SAE Brazil, São Paulo, SP (2001).

[3] M. Skorupa: Fatigue Fract. Engng. Mater. Struct. Vol. 21 (1998), p. 987.

[4] C.M. Ward-Close, A.F. Blom and R.O. Ritchie: Engng. Fract. Mech. Vol. 23 (1989), p. 613.

[5] D. Damri, J.F. Knott: Fatigue Fract. Engng. Mater. Struct. Vol. 14 (1991), p. 709.

[6] O.E. Wheeler: J. Basic Eng. Vol. 94 (1972), p. 181.

[7] D. Broek: *Elementary Engineering Fracture Mechanics* (Kluwer Academic Publishers, The Netherlands 1986).

[8] J. Willenborg, R.M. Engle and H.A. Wood, in: *AFFDL-TR71-1*, edited by Air Force Flight Dynamic Laboratory, USA (1971).

[9] T. H. Topper and D.L. DuQuesnay, in: *Modern Trends on Fatigue*, edited by P.M. Pimenta, L.C.H. Ricardo and A.F. Camarão / SAE Brazil, São Paulo, SP (2001).

[10] J.E. Allison, in: *ASTM STP 945*, edited by D.T. Reed and R.P. Reed / ASTM, Philadelphia, PA (1988).

[11] G.S. Wang and A.F. Blom: Eng. Fract. Mech. Vol. 40 (1991), p. 507.

[12] J. Schijve: *Fatigue of Structures and Materials* (Kluwer Academic Publishers, The Netherlands 2001).

[13] ASTM E647-01, in: *2001 Annual Book of ASTM Standards*, edited by American Society for Testing and Materials / ASTM, Philadelphia, PA (2001).

[14] R.G. Forman, V.E. Kearney and R.M. Engle: J. Basic Eng. Vol. 89 (1967), p. 459.

[15] A. F. Simões, in: *Effects of Overloading on Fatigue Crack Growth Retardation of an Al-7150 Alloy for Aeronautic Application*, M. Sc. Thesis. Rio de Janeiro, RJ (1997).

[16] X. Decoopman, A. Imad, M. Nait-Abdelaziz and G. Mesmacque, in: *Fracture from Defects*, edited M.W. Brown, E.R. de los Rios and K.J. Miller / Engineering Materials Advisory Services Ltd., Warley, UK (1998).